

Lanthanide nitrate complexes of the redox active ligand $(\eta^5\text{C}_5\text{H}_4\text{P}(\text{O})\text{Ph}_2)_2\text{Fe}$

Eileen Buckley-Dhoot^a, John Fawcett^b, Roman A. Kresinski^a, Andrew W.G. Platt^{c,*}

^aSchool of Chemical and Pharmaceutical Sciences, Kingston University, Penrhyn Road, Kingston-upon-Thames KT1 2EE, UK

^bDepartment of Chemistry, The University, Leicester LE1 7RH, UK

^cFaculty of Sciences, Staffordshire University, College Road, Stoke-on-Trent ST4 2DE, UK

ARTICLE INFO

Article history:

Received 22 October 2008

Accepted 24 February 2009

Available online 6 March 2009

Keywords:

Lanthanide nitrate

Ferrocene phosphine oxide

Structure

Electrochemistry

ABSTRACT

The synthesis of complexes of $(\eta^5\text{C}_5\text{H}_4\text{P}(\text{O})\text{Ph}_2)_2\text{Fe} = \text{L}$ with lanthanide nitrates is described. The single crystal X-ray structures for $\text{La}(\text{NO}_3)_3\text{L}(\mu\text{-L})\text{La}(\text{NO}_3)_3\text{L}$ (**1**), $[\text{Eu}(\text{NO}_3)_2\text{L}_2]_2[\text{Eu}(\text{NO}_3)_5]$ (**2**), $[\text{Ho}(\text{NO}_3)_2\text{L}_2]_2[\text{Ho}(\text{NO}_3)_5]$ (**3**) and $[\text{Lu}(\text{NO}_3)_2\text{L}_2]\text{NO}_3$ (**4**) are reported. Trends in Ln–O bond distances cannot be explained by the lanthanide contraction alone. The cyclic-voltammetric (CV) oxidation–reduction behaviour of **1**, **2**, **4** and $\text{Dy}(\text{NO}_3)_3\text{L}_2 \cdot 2\text{H}_2\text{O}$ is described. This was reversible on a timescale of a few seconds in all cases. In our hands the CV behaviour of **L** also seemed reversible on this timescale, although attempted chemical oxidation of **L** led to the isolation of $[\text{FeL}_2(\text{NO}_3)_2]\text{NO}_3$ (**5**) which was characterised by X-ray crystallography.

© 2009 Elsevier Ltd. All rights reserved.

1. Introduction

Several complexes of $(\eta^5\text{C}_5\text{H}_4\text{P}(\text{O})\text{Ph}_2)_2\text{Fe} = \text{L}$ with transition metals and their redox properties have been reported. These include complexes wherein **L** acts as a chelating ligand such as LPdCl_2 [**1**], LCoI_2 [**2**], $[\text{CuL}_2\text{EtOH}]^+$, $[\text{CuL}_2]^{2+}$ [**3**] and $\text{CuL}[(\text{C}_5\text{H}_4\text{PPh}_2)_2\text{Fe}]^+$ [**4**] and an example in which **L** bridges between metal centres in the polymeric $[\text{CoI}_2\mu\text{L}]_n$ [**2**]. In its oxidised form a complex with H^+ , $[\text{LH}][\text{Sb}_2\text{Cl}_8]$, has been reported [**5**]. There are no reports of complexes between lanthanide metals and the **L** ligand. The electrochemistry of substituted ferrocenes has been extensively studied [**6–8**], but there appear to be fewer studies on phosphine oxide substituted ferrocenes. Phosphine substituted ferrocene derivatives undergo ferrocene-based reversible oxidation followed by formation of the phosphine oxide [**9–11**]. Those such as **L** can be reversibly oxidised [**10**], whilst others such as $(\text{CpFeC}_5\text{H}_4)_2\text{P}(\text{O})\text{Ph}$ are irreversibly oxidised [**12**]. Similarly studies of the redox behaviour of phosphino and PO substituted ferrocene-based coordination complexes are sparsely reported. Complexes of $(\text{C}_5\text{H}_4\text{PPh}_2)_2\text{Fe}$ with Re are irreversibly oxidised [**13**] and $(\text{C}_5\text{H}_4\text{P}(\text{O})(\text{OEt})_2)_2\text{Fe} \cdot \text{ZnCl}_2$ undergoes oxidation at a potential very similar to the free ligand [**14**]. There being no reports of complexes between lanthanide metals and the **L** ligand, we were interested in their synthesis and structural and electrochemical properties.

2. Synthesis and properties

The complexes are readily prepared by direct reaction of the ligand with the appropriate lanthanide nitrate in ethanol solutions.

The complexes, which are all air and moisture stable, are sparingly soluble in ethanol but readily dissolve in CH_2Cl_2 and CHCl_3 . Solutions are stable over prolonged periods unlike those of the ligand itself which, although stable over periods of months in the dark, deposit insoluble brown solids on standing in sunlight for a few hours. Crystals of the complexes suitable for X-ray crystallography were obtained by slow diffusion of toluene into chloroform solutions of the complexes. Crystals were transferred to and handled under a dried mineral oil to minimise the deterioration of the crystals prior to data collection. The rapid solvent loss on exposure to normal laboratory conditions is probably responsible for elemental analyses which are consistent with the presence of fewer CHCl_3 molecules than found in the crystal structures. Attempted chemical oxidation of the ligand was investigated by reaction with Ag^+ with the aim of producing $[\text{L}]^+\text{NO}_3^-$. Stirring **L** with silver nitrate at room temperature in ethanol gave what appeared to be (by infrared spectroscopic evidence) an AgNO_3 complex of **L** with no redox reaction. Overnight reflux with AgNO_3 led to the formation of a dark brown solution from which was isolated the iron(III) complex $[\text{FeL}_2(\text{NO}_3)_2]\text{NO}_3$, characterised by single crystal X-ray crystallography.

3. Infrared spectroscopy

The infrared spectra show the expected features with two intense bands for the bidentate nitrate ligands and a shift to lower wavenumber of the PO stretching on complex formation. For the Lu complex the presence of the ionic nitrate is indicated by three medium intensity absorptions between those assigned to the chelated nitrate ligands. The absence of the expected band at $\sim 1390\text{ cm}^{-1}$ [**15**] is not without precedent; we have found that in lanthanide nitrate complexes of $\text{Ph}_2\text{P}(\text{O})\text{CH}_2\text{P}(\text{O})\text{Ph}_2$ [**16**] the

* Corresponding author.

E-mail address: A.Platt@staffs.ac.uk (A.W.G. Platt).

Table 1
Crystal data and structure refinement for the complexes 1–5.

Complex	1	2	3	4	5
Empirical formula	C108 H90 Cl18 Fe3 La2 N6 O24 P6	C148 H124 Cl36 Eu3 Fe4 N9 O35 P8	C150 H126 Cl42 Fe4 Ho3 N9 O35 P8	C68 H56 Fe2Lu N2 O10 P4	C68 H56 Fe3 N2 O10 P4
Formula weight	3125.16	4791.8	5069.45	1471.7	1352.58
Temperature (K)	150(2)	150(2)	150(2)	150(2)	150(2)
Wavelength (Å)	0.71073	0.71073	0.71073	0.71073	0.71073
Crystal system	triclinic	monoclinic	monoclinic	triclinic	triclinic
Space group	<i>P</i> 1	<i>C</i> 2/ <i>c</i>	<i>C</i> 2/ <i>c</i>	<i>P</i> 1	<i>P</i> 1
Unit cell dimensions	<i>a</i> = 12.982(7) Å <i>b</i> = 16.820(9) Å <i>c</i> = 19.634(11) Å	<i>a</i> = 31.509(3) Å <i>b</i> = 28.599(3) Å <i>c</i> = 23.677(2) Å	<i>a</i> = 31.356(3) Å <i>b</i> = 28.608(3) Å <i>c</i> = 23.647(2) Å	<i>a</i> = 12.682(2) Å <i>b</i> = 18.445(3) Å <i>c</i> = 19.542(3) Å	<i>a</i> = 12.888(3) Å <i>b</i> = 14.574(3) Å <i>c</i> = 18.439(4) Å
	$\alpha = 70.047(9)^\circ$ $\beta = 73.561(9)^\circ$ $\gamma = 70.107(7)^\circ$	$\alpha = 90^\circ$ $\beta = 110.530(3)^\circ$ $\gamma = 90^\circ$	$\alpha = 90^\circ$ $\beta = 110.697(3)^\circ$ $\gamma = 90^\circ$	$\alpha = 64.028(2)^\circ$ $\beta = 73.205(3)^\circ$ $\gamma = 76.209(3)^\circ$	$\alpha = 76.119(4)^\circ$ $\beta = 75.644(4)^\circ$ $\gamma = 80.810(4)^\circ$
Volume (Å ³)	3721(4)	19981(3)	19843(3)	3900.0(12)	3238.8(12)
Z	1	4	4	2	2
<i>D</i> _{calc} (Mg/m ³)	1.394	1.593	1.697	1.253	1.387
Absorption coefficient (mm ⁻¹)	1.293	1.821	2.164	1.754	0.821
<i>F</i> (000)	1560	9520	10032	1482	1392
Crystal size (mm)	0.28 × 0.19 × 0.15	0.23 × 0.12 × 0.10	0.35 × 0.14 × 0.11	0.25 × 0.21 × 0.10	0.29 × 0.22 × 0.20
θ range for data collection (°)	1.12–23.33	0.99–27.00	0.99–27.00	1.33–23.29	1.64–23.29
Index ranges	−14 ≤ <i>h</i> ≤ 14, −18 ≤ <i>k</i> ≤ 18, −21 ≤ <i>l</i> ≤ 21	−40 ≤ <i>h</i> ≤ 38, −36 ≤ <i>k</i> ≤ 36, −30 ≤ <i>l</i> ≤ 30	−39 ≤ <i>h</i> ≤ 39, −36 ≤ <i>k</i> ≤ 36, −29 ≤ <i>l</i> ≤ 30	−14 ≤ <i>h</i> ≤ 14, −20 ≤ <i>k</i> ≤ 20, −21 ≤ <i>l</i> ≤ 21	−14 ≤ <i>h</i> ≤ 14, −16 ≤ <i>k</i> ≤ 16, −20 ≤ <i>l</i> ≤ 20
Reflections collected	22911	83 615	82 304	24 421	20 229
Independent reflections [<i>R</i> _{int}]	10688 [0.0535]	21 769 [0.0996]	21 618 [0.1364]	11 201 [0.0228]	9296 [0.0225]
Completeness to θ (%)	98.9	99.8	99.8	99.90	99.4
Absorption correction	empirical	empirical	empirical	empirical	empirical
Max. and min. transmission	0.86 and 0.66	0.862 and 0.724	0.862 and 0.652	0.745 and 0.652	0.93 and 0.81
Refinement method	full-matrix least-squares on <i>F</i> ²	full-matrix least-squares on <i>F</i> ²	full-matrix least-squares on <i>F</i> ²	full-matrix least-squares on <i>F</i> ²	full-matrix least-squares on <i>F</i> ²
Data/restraints/parameters	10688/0/754	21 769/0/1096	21 618/0/1096	11 201/0/784	9296/0/784
Goodness-of-fit on <i>F</i> ²	1.043	0.861	0.890	0.993	1.059
Final <i>R</i> indices [<i>I</i> > 2 σ (<i>I</i>)]	<i>R</i> ₁ = 0.0672, <i>wR</i> ₂ = 0.1685	<i>R</i> ₁ = 0.0572, <i>wR</i> ₂ = 0.1160	<i>R</i> ₁ = 0.0613, <i>wR</i> ₂ = 0.1181	<i>R</i> ₁ = 0.0248, <i>wR</i> ₂ = 0.0590	<i>R</i> ₁ = 0.0345, <i>wR</i> ₂ = 0.0955
<i>R</i> indices (all data)	<i>R</i> ₁ = 0.0836, <i>wR</i> ₂ = 0.1760	<i>R</i> ₁ = 0.1090, <i>wR</i> ₂ = 0.1283	<i>R</i> ₁ = 0.1265, <i>wR</i> ₂ = 0.1377	<i>R</i> ₁ = 0.0280, <i>wR</i> ₂ = 0.0559	<i>R</i> ₁ = 0.0412, <i>wR</i> ₂ = 0.0987
Largest difference in peak and hole (e Å ⁻³)	1.883 and −1.513	1.683 and −0.842	1.457 and −1.126	0.940 and −0.646	0.366 and −0.267
Solvent accessible void (Å ³)	858.2	1805.4	1795	1129.9	460
Estimated solvent electron count	222e	476e	516e	290e	125e

interaction of “ionic” nitrate with H-bonding molecules can lead to infrared spectra which are essentially the same as for a coordinated nitrate.

4. Structures

4.1. General points

Details of the data collection and refinement for the crystal structures are given in Table 1 and selected bond lengths in Table 2.

The Ln–O distances show the effect of the lanthanide contraction showing a linear decrease in both Ln–O(N) and Ln–O(P) with decreasing ionic radius of the lanthanide as shown in Fig. 1. The Ln–O(N) distances are consistently longer than the Ln–O(P) which is a general feature of PO complexes with lanthanide nitrates. The magnitude of the difference in Ln–O(N) – Ln–O(P) (Δ) appears to reflect the degree of strain in the bonding region. Due to the strongly ionic nature of the interaction between the PO oxygen and the lanthanide ion a linear Ln³⁺–O[–]–P⁺ arrangement is favoured on electrostatic grounds. Values of Δ calculated from literature structures show that for non-chelated PO such as in Ln(NO₃)₃(Ph₃PO)_n [17] and Y(NO₃)₃(Ph₃PO)_n [18] values of Δ in the region of 0.21 Å are found. Constraining the PO in a six membered chelate ring in complexes such as Ln(NO₃)₃[(ⁱPrO)₂P(O)C₅H₄N(O)₂]₂ [19], Ln(NO₃)₃[(EtO)₂P(O)CH₂P(O)(OEt)₂]₂ [20] and Ln(NO₃)₃[(MeO)₂P(O)CMe(OH)P(O)(OMe)₂]₂ [21] lengthens the Ln–O(P) distance and hence reduces Δ to about 0.13–0.14 Å (interesting exceptions to this are complexes of Ph₂P(O)CH₂P(O)Ph₂ where a smaller Δ of 0.06 Å is observed [16]). Increasing the size of the chelate ring might be expected to increase the flexibility of the structure and allow Ln–O–P angles to approach linearity and thus values of Δ approaching those of an “unconstrained” ligand. Complexes with 10-membered chelate rings 1,3-[Ph₂P(O)]₂C₆H₄ [22] do indeed show this effect with Δ of 0.21 Å. In this study, a value of Δ = 0.22 Å is found, again implying relatively unconstrained coordination of the PO groups. This is further seen in the values of the Ln–O–P angles which average 161.8° (range 152.3–177.3°) over all the lanthanide complexes reported here.

It has been previously observed that small bite angle ligands such as nitrate should preferentially bind to larger metal ions [23]. Although it should be noted that all the metals here fall in to the category of large ions it is still interesting in this respect to examine the changes in Ln–O bond distances. When the Ln–O(N) distances are corrected for the lanthanide contraction, by subtracting the ionic radius of the lanthanide ion with the appropriate coordination number [24], the difference should be constant if no other effects are significant. Single factor Anova analysis of the data reveals that significant differences occur between the sets of distances. Post hoc analysis of the results was carried out by un-

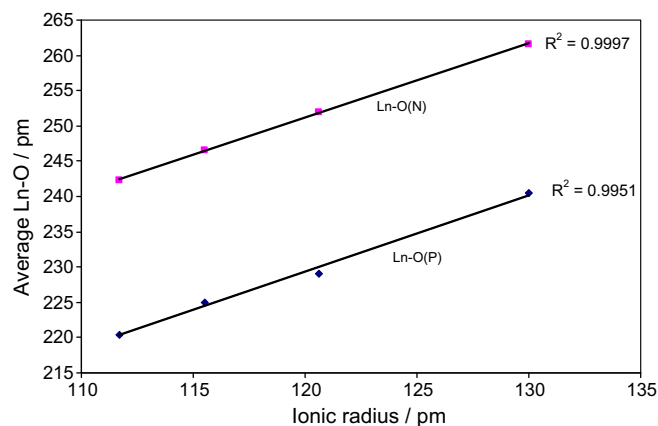


Fig. 1. The relationship between the Ln–O(P) and Ln–O(N) distances and the ionic radius of the lanthanide ion for complexes 1–4.

paired *t*-test assuming a null hypothesis of no difference between the means and unequal variance at a 95% confidence level. The results of such an analysis show that there are significant differences between the La–O(N) and other Ln–O distances, with La–O(N) being shorter than expected. The differences between the Eu–O(N), Ho–O(N) and Lu–O(N) are not significant once the effect of the lanthanide contraction is taken into account. The average Ln–O distances corrected for the lanthanide ion size are significantly larger for the Eu and Ho complexes. In the Eu and Ho complexes the larger residual differences with averages of 1.314(2) Å, compared with 1.256(2) Å for the La and Lu complexes, can be ascribed to the hydrogen bonding between chloroform and the coordinated nitrate ions. In the La complex this interaction is considerably weaker with a shortest (N)O...HCCl₃ of 2.547 Å compared with 2.246 and 2.232 Å, respectively, for the Eu and Ho complexes and this may in part account for the stronger La–O interaction. There are short contacts between one of the H atoms on the cyclopentadiene ring and one of the O(N) atoms in all the complexes. These distances, in the region of 2.3 Å, are shorter than the sum of van der Waals radii of O and H (2.60 Å), but, as such interactions occur in all complexes, they cannot account for the variations in distances observed.

A similar analysis for the Ln–O(P) distances for the chelate rings reveals significant differences between the La–O(P) distances and those for the other complexes. The values of Ln–O(P) corrected for the size of the lanthanide ion, again indicate a stronger La–O interaction with residual distances of 1.048 Å for La and 1.085, 1.094 and 1.087 Å for the Eu, Ho and Lu complexes respectively. It is difficult to see a reason for this. The non-bonded (P)O...O(P) distances within the chelate rings are larger for the Eu and Ho complexes (3.262 (Eu) and 3.212 Å (Ho) compared with 3.160 and

Table 2
Selected bond lengths for the lanthanide complexes.

	La		Eu	Ho	Lu	Fe
La(1)–O(2)	2.403(5)	Ln(1)–O(2)	2.276(4)	2.232(4)	2.2043(18)	1.9753(19)
La(1)–O(1)	2.406(5)	Ln(1)–O(1)	2.283(4)	2.240(4)	2.2152(19)	1.9713(19)
La(1)–O(3)	2.425(5)	Ln(1)–O(4)	2.303(4)	2.258(4)	2.2008(19)	1.9749(18)
La(1)–O(11)	2.591(5)	Ln(1)–O(3)	2.302(4)	2.266(4)	2.1962(19)	1.9814(19)
La(1)–O(8)	2.592(6)	Ln(1)–O(9)	2.490(4)	2.428(5)	2.4158(19)	
La(1)–O(5)	2.593(5)	Ln(1)–O(5)	2.523(4)	2.467(5)	2.4183(19)	2.0458(19)
La(1)–O(7)	2.632(6)	Ln(1)–O(6)	2.523(4)	2.468(4)	2.434(2)	
La(1)–O(4)	2.632(5)	Ln(1)–O(8)	2.542(4)	2.497(5)	2.423(2)	2.0120(19)
La(1)–O(10)	2.654(5)					
P(1)–O(1)	1.495(5)		1.504(4)	1.492(5)	1.496(2)	1.517(2)
P(2)–O(2)	1.496(5)		1.501(4)	1.501(5)	1.4935(19)	1.502(2)
P(3)–O(3)	1.503(5)		1.492(4)	1.488(4)	1.502(2)	1.500(2)
P(4)–O(4)			1.499(4)	1.493(5)	1.496(2)	1.4987(19)

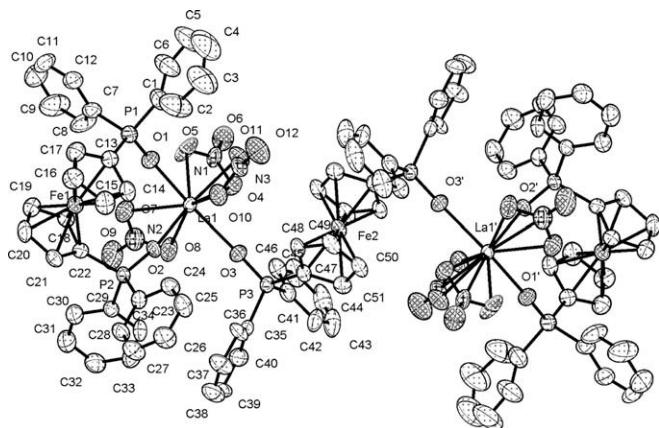


Fig. 2. The structure of $[\text{La}(\text{NO}_3)_3]_2\mu\text{-L}$. The Fe2 atom is located on a centre of symmetry. Symmetry related atoms generated by $1 - x, 1 - y, -z$.

3.175 Å for the La and Lu complexes, respectively) implying smaller electrostatic repulsions, which in turn suggests that stronger binding to the metal might be possible. The other obvious candidate for repulsive interactions which might lead to a weakening of the Ln–O(P) bonds are the non-bonded interactions between the (P)O and (N)O atoms. Significant differences are also indicated by single factor Anova analysis for the non-bonded P(O)⋯O(N) distances. A post hoc analysis of the non-bonded P(O)⋯O(N) distances by *t*-tests between the pairs of complexes shows a trend of increasing significance in the differences of the means. The differences between the La and Eu, complex is only significant at an 88.3% confidence level, whilst this increases to 98.9% and 99.9% for the differences between the La complex and the Ho and Lu complexes, respectively. For the La complex the shortest of these non-bonded interactions is over 3 Å whilst for all the others it is lower, showing a trend in values of 2.885 (Eu), 2.814 (Ho) and 2.768 Å (Lu). This trend mirrors the confidence levels at which the differences in the P(O)⋯O(N) means between the La complex and the respective sets of distances for the other complexes become significant.

The structures of the complexes have a number of features in common. The twist angles of the cyclopentadiene rings, measured from the torsional angles between the vectors from the ring centroid and ring carbon atoms on corresponding positions of the two rings, vary depending on whether the ligand is chelating or bridging. In the bridging mode observed in the lanthanum complex, the ligand is able to adopt a similar structure to that of the free ligand itself, namely with staggered rings and the diphenylphosphine oxide groups in a *trans* arrangement. Here the twist angle between the rings averages at $38.0 \pm 0.7^\circ$, which is in good agreement with the average values of $37.7 \pm 0.5^\circ$ in the free ligand [25], $36.1 \pm 1.5^\circ$ found in the polymeric form of CoL_2L [2], and $26.6 \pm 0.9^\circ$ found for the bridging ligands in the zinc chloride complex of $[\text{C}_5\text{H}_4\text{P}(\text{O})(\text{OEt})_2]_2\text{Fe}$ [14]. The formation of chelate rings imposes a more eclipsed conformation on the ferrocenyl nucleus. The twist angles for the chelating ligands in the complexes are similar, with those in the lanthanum complex averaging at $8.6 \pm 0.4^\circ$ with averages of $12.8 \pm 0.6^\circ$ and $5.9 \pm 0.5^\circ$ (Eu), $12.1 \pm 0.8^\circ$ and $5.6 \pm 0.3^\circ$ (Ho) and $6.8 \pm 0.3^\circ$ and $4.5 \pm 0.3^\circ$ (Lu). These values are similar to that found in PdCl_2L ($7.3 \pm 1.4^\circ$) but larger than observed in monomeric form of CoL_2L which has an average twist angle of $1.8 \pm 0.6^\circ$.

4.2. The structure of $\text{LLa}(\text{NO}_3)_3\text{-}\mu\text{L-La}(\text{NO}_3)_3\text{L}$ (1)

The lanthanum nitrate complex (1) crystallised as a dimer, $\text{LLa}(\text{NO}_3)_3\text{-}\mu\text{L-La}(\text{NO}_3)_3\text{L}$ in which each La is nine coordinate. The structure is shown in Fig. 2. The coordination geometry does not

conform to any simple polyhedron, but can be considered as a somewhat distorted octahedron if the nitrates are visualised as monodentate ligands bonded via the N-atoms. The octahedron thus conceptualised is a *mer*-isomer with “*cis*” angles at La averaging $92.4 \pm 9.3^\circ$ whilst the corresponding “*trans*” angles average $162.1 \pm 9.4^\circ$. The La–O(P) distances for the chelating phosphine oxide are essentially identical (2.404(5) Å) and shorter than that from the bridging PO group (2.425(5) Å). These differences are not reflected in the PO distances themselves which are apparently equal at 1.4978(5) Å regardless of whether the PO groups are in the chelating or bridging mode. The nitrate groups bond asymmetrically to the lanthanum ion with one short and one long La–O distance, with averages of 2.592(8) and 2.639(10) Å, respectively. These differences are reflected in the bond distances within each nitrate ion itself, with a short O–N distance (1.254(6) Å) corresponding to the short La–O and the longer N–O associated with the longer La–O (1.276(9) Å). The P–O–La angles approach the idealised linear geometry for all the phosphoryl groups, as expected for predominantly ionic bonding where the structure imposes relatively few constraints on ligand architecture.

4.3. The structures of $[\text{Eu}(\text{NO}_3)_2\text{L}_2]_2[\text{Eu}(\text{NO}_3)_5]$ (2), $[\text{Ho}(\text{NO}_3)_2\text{L}_2]_2[\text{Ho}(\text{NO}_3)_5]$ (3) and $[\text{Lu}(\text{NO}_3)_2\text{L}_2][\text{NO}_3]$ (4)

In general, the reduction of the ionic radius tends to lower the coordination number of the metal. The cations in these complexes have eight-coordinate lanthanide ions and are rather similar in motif; the structure of the cation in 2 is shown as a representative example in Fig. 3. The coordination geometries can be visualised as distorted octahedra if the nitrate ions are considered as pseudomonodentate ligands attached via the N-atom. The *trans*-N–Ln–N angles are $176.21(15)^\circ$ (Eu), $176.63(17)^\circ$ (Ho) and $177.53(7)^\circ$ (Lu) whilst the average corresponding *trans*-O–Ln–O angles are $163.6 \pm 0.3^\circ$, $162.9 \pm 0.4^\circ$ and $164.9 \pm 4.1^\circ$. The *cis*-N–Ln–O angles give averages close to 90° , at $90.1 \pm 8.5^\circ$ (Eu), $90.0 \pm 8.7^\circ$ (Ho) and $90.0 \pm 10.1^\circ$ (Lu) whilst the *cis*-O–Ln–O angles are rather more uniform with averages of $91.2 \pm 1.0^\circ$, $91.3 \pm 0.8^\circ$ and $91.7 \pm 0.8^\circ$ for Eu, Ho and Lu, respectively. The $\text{Ln}(\text{NO}_3)_5^{2-}$ ions contain 10-coordinate lanthanide ions but are readily envisaged as trigonal bipyramids,

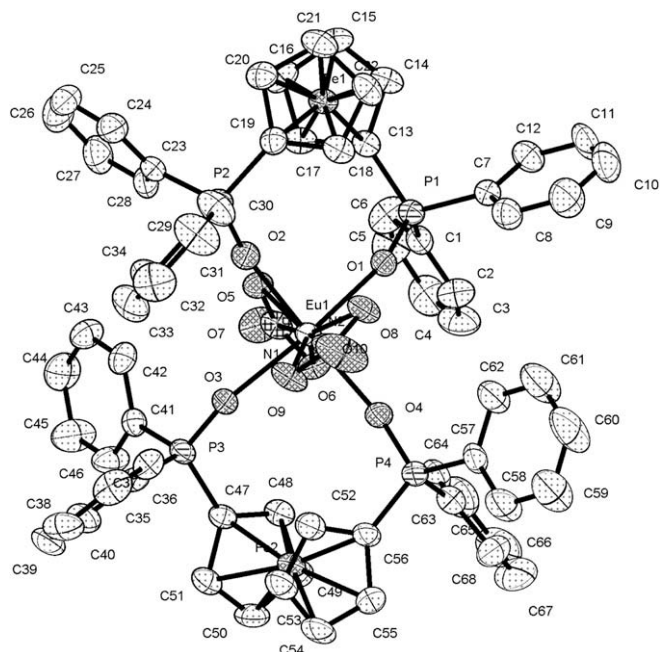


Fig. 3. The cation in $[\text{Eu}_2(\text{NO}_3)_2]_2[\text{Eu}(\text{NO}_3)_5]^{2-}$.

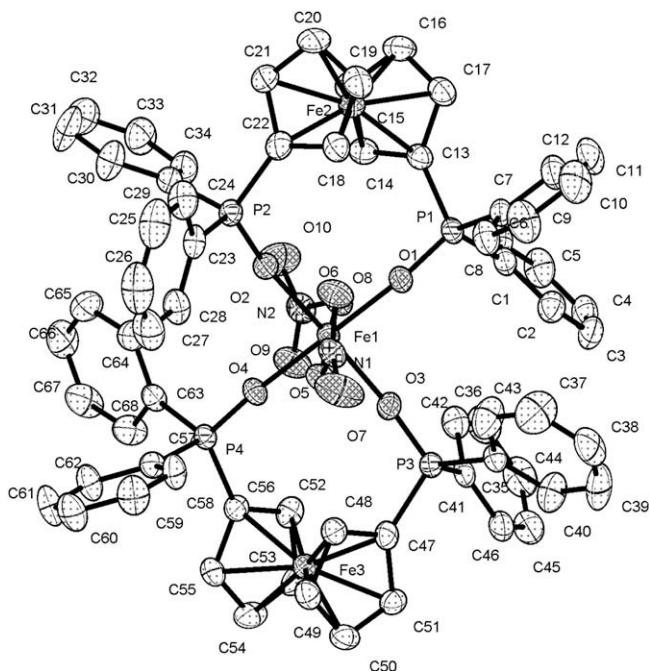


Fig. 4. The structure of $[\text{FeL}_2(\text{NO}_3)_2]\text{NO}_3$.

again taking the nitrate ions as pseudomonodentate ligands. The equatorial nitrogen atoms and the lanthanide ion are coplanar in both structures, the $N_{\text{ax}}\text{-Ln}\text{-}N_{\text{ax}}$ angles are 177.9° , the $N_{\text{eq}}\text{-Ln}\text{-}N_{\text{eq}}$ average to 120.0° (range $118.77\text{--}122.45^\circ$) whilst the $N_{\text{eq}}\text{-Ln}\text{-}N_{\text{ax}}$ angles average at $91.7 \pm 5.3^\circ$ and $90.0 \pm 6.2^\circ$ for the Eu and Ho complexes, respectively. There are many examples of $\text{Ln}(\text{NO}_3)_5^{2-}$ counter-ions in the literature [26].

4.4. The structure of $[\text{FeL}_2(\text{NO}_3)_2]\text{NO}_3$

The structure of $[\text{FeL}_2(\text{NO}_3)_2]\text{NO}_3$ (**5**) is shown in Fig. 4 and shows interesting differences with the Lu complex with which it is superficially analogous. The iron is six-coordinate with the nitrate ions bound in a monodentate manner. The geometry about the metal is essentially octahedral with the *trans*-O-Fe-O angles averaging at $177.1 \pm 1.1^\circ$ and the *cis*-O-Fe-O at $90.0 \pm 3.3^\circ$. The cyclopentadiene rings are eclipsed with twist angles of $2.6 \pm 0.5^\circ$ and $0.3 \pm 0.1^\circ$ for the two ligands. The P-O-Fe angles have a slightly larger range than the corresponding angles in the lanthanide complexes with one ligand having angles approaching linearity, whilst the other is significantly bent. This seems to have little effect on the Fe-O or P-O distances which are in essence independent of the angle at the oxygen atoms.

5. Mass spectrometry

Electrospray mass spectra were recorded for all the complexes in CH_2Cl_2 . The base peak in all cases is $[\text{L}+\text{H}]^+$. The loss of a single nitrate to give $[\text{LnL}_2(\text{NO}_3)_2]^+$ is observed for all the complexes generally as a low intensity signal. The most notable feature of the mass spectra is the presence of ions formed as the result of ligand redistribution reactions. Thus signals of significant intensity are observed for ions such as $[\text{LnL}_4]^{3+}$ (5–10%), $[\text{LnL}_3]^{3+}$ (70–10%), $[\text{LnL}_3(\text{NO}_3)]^{2+}$ (40–5%) and $[\text{LnL}(\text{NO}_3)]^{2+}$ (10–30%). Some trends in the relative intensities of the signals from the ions are explicable by the lanthanide contraction. Thus the intensity of the peak assigned as $[\text{LnL}_3]^{3+}$ decreases from 70% for La to 10% for the Yb com-

Table 3
Peak potentials^a for selected complexes.

	1	2	$\text{Dy}(\text{NO}_3)_3\text{L}_2 \cdot 2\text{H}_2\text{O}$	4
$E_{1/2}$ (complex) (mV) ^b	628	661	681	683
ΔE (ferrocene) (mV)	70	77	70	78
ΔE (complex) (mV)	57	66	75	83

^a Relative to ferrocene as internal reference.

^b All peak potentials are measured with respect to ferrocene using a pseudoreference Ag wire.

plex. Similarly the intensity of the peak due to $[\text{LnL}_3(\text{NO}_3)]^{2+}$ decreases from 40% (La) to below 5% (Yb) reflecting the increased steric interactions as the ionic radius decreases.

The negative ion spectra of the complexes showed a base peak at $m/z = 62.1$ assigned as NO_3^- and no other peaks of significant intensity. A much lower intensity signal (<1%) at $m/z = 648$ which is assigned as $[\text{L}+\text{NO}_3]^-$. There were no observed peaks which could be assigned to species such as $\text{Ln}(\text{NO}_3)_4^-$ or $\text{Ln}(\text{NO}_3)_5^{2-}$. Such species might have been anticipated given the solid state structures of the Ho and Eu complexes.

6. Cyclic voltammetry

The oxidation behaviour of **1**, **2**, $\text{Dy}(\text{NO}_3)_3\text{L}_2 \cdot 2\text{H}_2\text{O}$ and **4** was studied by cyclic voltammetry in 0.1 M Bu_4NClO_4 solution in acetonitrile, with ferrocene as internal standard. Ligand L and each complex display a single reversible oxidation event corresponding to each {L} unit; in no case is any other wave evident, such as might suggest inequivalent L environments, or any degree of electronic communication between equivalent environments. Nevertheless, in the case of **1**, we clearly have a case of a complex which possesses inequivalent L environments in the solid state. We can offer no explanation for the single redox wave, other than a solution fluxionality or lability of the complex over the approximate 700 ms duration of the oxidation and re-reduction waves. All complexes, as written above, display a continuous shift toward more positive oxidation potentials with atomic number (Table 3). Ligand L itself is shifted some +458 mV with respect to ferrocene in good agreement with the literature value of +430 mV afforded by a previous determination in a different solvent system [10]. The Ln complexes follow a clear pattern which offers evidence for a closely associated molecular complex between Ln and L, albeit fluxional, being present in solution in each case. The trend is consistent with increasing polarising power of the smaller lanthanide metals drawing electron density onto the O atoms of the L ligand and away from the Fe centre. We attempted to reduce the Eu complex **2** in the same electrolyte solution after deoxygenation by nitrogen sparging, but no reduction peaks were observed in the potential window of the solvent/electrolyte system used.

7. Experimental

7.1. Crystallography

Crystals were transferred to and handled under a dried mineral oil to minimise the deterioration of the crystals prior to data collection. All X-ray data for the complexes were measured on a Bruker SMART diffractometer with a 2 K CCD area detector using graphite monochromated $\text{Mo K}\alpha$ radiation ($\lambda = 0.71073 \text{ \AA}$). Absorption corrections, based on comparison of Laue equivalents, were applied to the data sets. The structures were solved by Patterson methods and refined by full-matrix least-squares cycles on F^2 for all data, using SHELXTL [27]. All non-hydrogen atoms of the metal complexes were refined with anisotropic displacement parameters and all

hydrogen atoms were included in refinement cycles riding on bonded atoms. For all structures the metal complex was unambiguous and refined satisfactorily. For **1**, **2** and **3** lattice CHCl_3 was located and refined. However, all the structures were found to have regions of unresolved disordered solvent, thought to be CHCl_3 , that could not be modelled satisfactorily. The SQUEEZE option of the programme PLATON [28] was used to omit the data for the disordered regions for each of the structures. The solvent accessible void volume and estimated solvent electron count for each structure is given in Table 1.

7.2. Infrared spectroscopy

Infrared spectra were recorded on a Thermo Nicolet Avatar 370 FT-IR spectrometer operating in ATR mode. Samples were compressed onto the optical window and spectra recorded without further sample pre-treatment.

7.3. Electrospray mass spectrometry

Electrospray mass spectra were obtained by the EPSRC National Mass Spectrometry Service Centre at Swansea University as described previously [29]. The spectra were recorded on a VG Quattro II triple quadrupole mass spectrometer. Samples dissolved in CH_2Cl_2 were loop injected into a stream of MeOH passing through a steel capillary held at high voltage (+3.5 kV for positive mode and -3.0 kV for negative mode). Nebulisation of the resulting spray was pneumatically assisted by a flow of nitrogen bath gas and heated source (70 °C). Declustering and molecular fragmentation were promoted by increasing the cone voltage from 8 to 50 V.

7.4. Electrochemistry

The oxidation behaviour of L, **1**, **2**, $\text{Dy}(\text{NO}_3)_3\text{L}_2 \cdot 2\text{H}_2\text{O}$ and **4** was studied using a PC-driven Bioanalytical Systems BAS100B Electrochemical Analyzer/BAS PA1 Pre-amplifier combination operating in cyclic voltammetry mode with a sweep width of 1400 mV and sweep rate of 200 mV s^{-1} . The working electrode was polished Pt disc, the auxiliary electrode Pt wire and the pseudoreference electrode Ag wire. Approximately 1–5 mg samples were dissolved in approximately 20 ml of 0.1 M Bu_4NClO_4 in acetonitrile solution, with ferrocene as internal standard. Commercial white-spot nitrogen was used as spargent for reduction experiments.

7.5. Synthesis

$(\text{C}_5\text{H}_4\text{P}(\text{O})\text{Ph}_2)_2\text{Fe}$: $(\text{C}_5\text{H}_4\text{PPh}_2)_2\text{Fe}$ (5.17 g) was suspended in 50 ml acetone and H_2O_2 (3.00 g 30% aqueous solution) slowly added at such a rate as to maintain a gentle reflux. The suspension was stirred overnight, filtered and the resulting yellow solid washed with a little acetone and diethyl ether and dried at the pump to give 5.31 g (93% as the hydrate) yellow powder. Infrared/ cm^{-1} (ATR) ν_{PO} 1165(s) ν_{OH} 3409(m).

$[\text{La}(\text{NO}_3)_3\text{L}_2]_2\text{L}_3 \cdot 1.5\text{CHCl}_3$: $\text{La}(\text{NO}_3)_3\text{L}_2 \cdot 6\text{H}_2\text{O}$ (0.38 g 0.87 mmol) in 3 ml EtOH was added in portions to a solution of L (0.25 g 0.42 mmol) in 5 ml hot EtOH. A yellow-brown precipitate was formed on each addition. On cooling, the yellow-brown solid formed, and was filtered, washed with a little EtOH and dried at the pump to yield 0.23 g. Crystals suitable for X-ray analysis were grown by slow diffusion of toluene into a CHCl_3 solution to give dark brown crystals.

Infrared (ATR) ν_{NO} 1436(s) 1295(s), ν_{PO} 1138(s). *Anal. Calc.*: C, 48.03; H, 3.33; N, 3.25. *Found*: C, 47.88; H, 3.39; N, 3.51%.

$[\text{Eu}(\text{NO}_3)_3\text{L}_2]_2[\text{Eu}(\text{NO}_3)_5]_2 \cdot 2.5\text{CHCl}_3$: $\text{Eu}(\text{NO}_3)_3\text{L}_2 \cdot 6\text{H}_2\text{O}$ (0.29 g, 0.65 mmol) in 2 ml EtOH was added in portions to a solution of L (0.32 g, 0.55 mmol) in 3 ml hot EtOH as for the La complex above and gave 0.41 g yellow-brown powder. Crystals for X-ray analysis

grown by slow diffusion of toluene into a CHCl_3 solution rapidly lost solvent on exposure to air.

Infrared/ cm^{-1} (ATR) ν_{NO} 1473(s) 1282(s), ν_{PO} 1142(s). *Anal. Calc.* for $[\text{Eu}(\text{NO}_3)_3\text{L}_2]_2[\text{Eu}(\text{NO}_3)_5]_2 \cdot 2.5\text{CHCl}_3$: C, 45.48; H, 3.16; N, 3.45. *Found*: C, 45.11; H, 3.66; N, 3.81%.

$[\text{Ho}(\text{NO}_3)_3\text{L}_2]_2[\text{Ho}(\text{NO}_3)_5]_2 \cdot 2\text{CHCl}_3$: $\text{Ho}(\text{NO}_3)_3\text{L}_2 \cdot 6\text{H}_2\text{O}$ (0.32 g, 0.70 mmol) in 2 ml EtOH was added in portions to a solution of L (0.30 g, 0.50 mmol) in 3 ml hot EtOH as for the La complex above gave 0.24 g yellow-brown powder. Crystals for X-ray analysis grown by slow diffusion of toluene into a CHCl_3 solution rapidly lost solvent on exposure to air.

Infrared/ cm^{-1} (ATR) ν_{NO} 1473(s) 1287(s), ν_{PO} 1146(s). *Anal. Calc.* for $[\text{Ho}(\text{NO}_3)_3\text{L}_2]_2[\text{Ho}(\text{NO}_3)_5]_2 \cdot 2\text{CHCl}_3$: C, 45.57; H, 3.16; N, 3.47. *Found*: C, 45.37; H, 3.24; N, 3.63%.

$\text{Dy}(\text{NO}_3)_3\text{L}_2 \cdot 2\text{H}_2\text{O}$: A solution of $\text{Dy}(\text{NO}_3)_3\text{L}_2 \cdot 6\text{H}_2\text{O}$ (0.12 g) in 1.0 ml EtOH was added to a solution of L (0.36 g) in 2 ml EtOH. A yellow-brown precipitate formed on each addition. On complete addition the solid was filtered, washed with EtOH and dried at the pump (0.25 g).

Infrared (ATR) ν_{NO} 1477(s) 1283(s), ν_{PO} 1142(s). *Anal. Calc.*: C, 52.45; H, 3.88; N, 2.70. *Found*: C, 52.08; H, 3.79; N, 2.54%.

$\text{Lu}(\text{NO}_3)_3\text{L}_2 \cdot 2\text{H}_2\text{O}$: A solution of $\text{Lu}(\text{NO}_3)_3\text{L}_2 \cdot 6\text{H}_2\text{O}$ (0.10 g) in 1.5 ml EtOH was added to a solution of L (0.27 g) in 10 ml EtOH. On reduction of the volume of the solution to about 5 ml brown crystals were deposited which were filtered washed with EtOH and dried at the pump to give the product (0.25 g).

Infrared/ cm^{-1} (ATR) ν_{OH} 3400(w) ν_{NO} 1499(s) 1482(s) 1359(m) 1337(m) 1307(m) 1288(s), ν_{PO} 1152(s). *Anal. Calc.*: C, 52.03; H, 3.85; N, 2.68. *Found*: C, 52.30; H, 3.81; N, 2.74%.

$\text{Fe}(\text{NO}_3)_2\text{L}_2\text{NO}_3 \cdot 3.5\text{H}_2\text{O}$: A solution of L (2.01 g) and silver nitrate (1.03 g) in 40 ml ethanol was heated under reflux for 8 h. The solution was cooled, filtered and allowed slowly to evaporate to 25 ml when dark brown crystals formed. These were filtered, washed with a small quantity of ethanol, and dried at the pump to give dark brown crystals (0.59 g).

Infrared/ cm^{-1} ν_{OH} 3389(w) ν_{NO} 1489(m), 1488(m), 1481(m), 1280(s), ν_{PO} 1135(s), 1120(s). *Anal. Calc.*: C, 55.25; H, 4.30; N, 2.84. *Found*: C, 55.30; H, 4.50; N, 2.94%.

Supplementary data

CCDC 620324–620328 contains the supplementary crystallographic data for Fe, La, Eu, Ho and Lu structures, respectively. These data can be obtained free of charge via <http://www.ccdc.cam.ac.uk/conts/retrieving.html>, or from the Cambridge Crystallographic Data Centre, 12 Union Road, Cambridge CB2 1EZ, UK; fax: (+44) 1223-336-033; or e-mail: deposit@ccdc.cam.ac.uk.

Acknowledgements

We are grateful to the Royal Society of Chemistry for support from the research fund and the EPSRC for use of the National Mass Spectrometry Service at Swansea University.

References

- [1] J.S.L. Yeo, J.J. Vittal, T.S.A. Hor, *J. Chem. Soc., Chem. Commun.* (1999) 1477.
- [2] T. Aviles, A. Dinis, J. Orlando Gonçalves, V. Felix, M.J. Calhorda, A. Prazeres, M.G.B. Drew, H. Alves, R.T. Henriques, V. da Gama, P. Zanello, M. Fontana, *J. Chem. Soc., Dalton Trans.* (2002) 4595.
- [3] G. Pilloni, G. Valle, C. Corvaja, B. Longato, B. Corain, *Inorg. Chem.* 34 (1995) 5910.
- [4] G. Pilloni, B. Corain, M. Degano, B. Longato, G. Zanotti, *J. Chem. Soc., Dalton Trans.* (1993) 1777.
- [5] I.A. Razak, U. Usman, H.-K. Fun, B.M. Yamin, N.A.M. Kasim, *Acta Crystallogr., Sect. C* 58 (2002) 225.
- [6] M. Emília, N.P.R.A. Silva, A.J.L. Pombeiro, J.J.R. Fraústo da Silva, R. Herrmann, N. Deus, T.J. Castilho, M. Fátima, C.G. Silva, *J. Organomet. Chem.* 421 (1991) 75.

- [7] M. Emília, N.P.R.A. Silva, A.J.L. Pombeiro, J.J.R. Fraústo da Silva, R. Herrmann, N. Deus, R.E. Bozak, *J. Organomet. Chem.* 480 (1994) 81.
- [8] W.L. Davis, R.F. Shago, E.H.G. Langner, J.C. Swart, *Polyhedron* 24 (2005) 1611.
- [9] J. Podlaha, P. Stepnicka, J. Ludvik, I. Cisarova, *Organometallics* 15 (1996) 543.
- [10] G. Pilloni, B. Longato, B. Corain, *J. Organomet. Chem.* 420 (1991) 57.
- [11] P. Zanello, G. Opromolla, G. Giorgi, G. Sasso, A. Togni, *J. Organomet. Chem.* 506 (1996) 61.
- [12] D.A. Durfey, R.U. Kirss, C. Frommen, W. Feighery, *Inorg. Chem.* 39 (2000) 3506.
- [13] T.M. Miller, K.J. Ahmed, M.S. Wrightson, *Inorg. Chem.* 28 (1989) 2347.
- [14] O. Oms, F. Maurel, F. Carré, J. le Bideau, A. Vioux, D. Leclercq, *J. Organomet. Chem.* 689 (2004) 2654.
- [15] K. Nakamoto, *Infrared and Raman Spectra of Inorganic and Coordination Compounds*, 5th Ed., Wiley, 1997.
- [16] A.M.J. Lees, A.W.G. Platt, *Inorg. Chem.* 42 (2003) 4673.
- [17] W. Levason, E.H. Newman, M. Webster, *Polyhedron* 19 (2000) 2697.
- [18] L. Deakin, W. Levason, M.C. Popham, G. Reid, M. Walker, *J. Chem. Soc., Dalton Trans.* (2000) 2439.
- [19] G.S. Conary, A.A. Russell, R.T. Paine, J.H. Hall, R.R. Ryan, *Inorg. Chem.* 27 (1988) 3242.
- [20] A.M.J. Lees, R.A. Kresinski, A.W.G. Platt, *New J. Chem.* 28 (2004) 1457.
- [21] A.M.J. Lees, J.M. Charnock, R.A. Kresinski, A.W.G. Platt, *Inorg. Chim. Acta* 312 (2001) 170.
- [22] Y.-C. Tan, X.-M. Gan, J.C. Stanchfield, E.N. Duesler, R.T. Paine, *Inorg. Chem.* 40 (2001) 2910.
- [23] R.D. Hancock, A.E. Martell, *Chem. Rev.* 89 (1989) 1875.
- [24] R.D. Shannon, *Acta Crystallogr.* A32 (1972) 751.
- [25] Z.-G. Fang, T.S.A. Hor, Y.-S. Wen, L.-K. Liu, T.C.W. Mak, *Polyhedron* 14 (1995) 2403.
- [26] F.H. Allen, *Acta Crystallogr.* B58 (2002) 380.
- [27] SHELXTL, An Integrated System for Solving, Refining and Displaying Crystal Structures, Version 5.10, Bruker Analytical X-ray Systems, Madison, WI, USA, 1997.
- [28] A.L. Spek, PLATON, Version 1.5, A Multi-Purpose Crystallographic Tool, Utrecht University, Utrecht, The Netherlands, 2002.
- [29] J. Fawcett, A.W.G. Platt, D.R. Russell, *Polyhedron* 21 (2002) 287.